DOI: 10.1002/anie.201102321

Tellurium Compounds

An Iridium-Stabilized, Formally Uncharged Te_{10} Molecule with 3-Center–4-Electron Bonding**

Anja Günther, Martin Heise, Frank R. Wagner, and Michael Ruck**

In contrast to the lighter homologues sulfur and selenium, molecular allotropes of tellurium are not known. Yet, the crown-shaped Te_8 rings in $Cs_3Te_6(Te_8)_2$[1] and $Cs_4Te_{20}(Te_8)$[2] provided first evidence that uncharged tellurium rings can be stabilized in the solid state. Further homonuclear species were reported, such as Te_4 in $[Te_4\{Cr(CO)_5\}_4]$[3] or Te_6 in $Re_6Te_{10}Cl_6(Te_6)$[4] and $(AgI)_2(Te_6)$.[5] Recently, a new binding mode, where formally uncharged tellurium molecules act as electron-pair donors for transition metals, was reported for the coordination polymers $[Ru(Te_9)](InCl_4)_2$, $[Ru(Te_8)]Cl_2$, and $[Rh(Te_6)]Cl_3$.[6] A much broader structural chemistry of tellurium is observed in its polyanionic[7] and polycationic[8] forms demonstrating also the ability of Te atoms to feature 3-center–4-electron (3c–4e) bonding. Such "hypervalent" atoms are found, for example, in polyanions Te_5^{6-},[8] $^1_\infty[Te_3^{2-}]$,[7a] and $(TePh)_3^-$,[9] in the polycation $^1_\infty[Te_7^{2+}]$,[10] or in extended uncharged structures, such as β-TeI,[11] and $(Te_2)_2I_2$[12] (Figure 1).

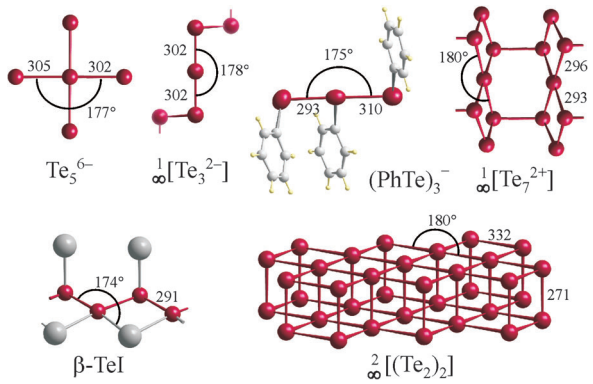

Figure 1. Examples for Te species with 3c–4e bonds (distances in pm).

[*] A. Günther, M. Heise, Prof. Dr. M. Ruck
Department of Chemistry and Food Chemistry
Dresden University of Technology, 01062 Dresden (Germany)
E-mail: michael.ruck@tu-dresden.de
Dr. F. R. Wagner, Prof. Dr. M. Ruck
Max Planck Institute for Chemical Physics of Solids
Nöthnitzer Strasse 40, 01187 Dresden (Germany)
E-mail: wagner@cpfs.mpg.de

[**] We gratefully acknowledge Dr. S. Hoffmann and Dr. W. Schnelle (MPI CPfS) for TG-MS, magnetic susceptibility and electrical resistivity measurements. This work was supported by the Deutsche Forschungsgemeinschaft (DFG).

Supporting information for this article is available on the WWW under http://dx.doi.org/10.1002/anie.201102321.

With $Ir_2Te_{14}Cl_{14}$ (**1**) we now isolated a tellurium-rich compound that contains for the first time an uncharged Te molecule with 3c–4e bonding. Compound **1** was obtained in high yield by the reaction of Ir, Te, and $TeCl_4$ at 250 °C. X-ray diffraction on a single crystal revealed a triclinic packing of C_i-symmetric $(Te_{10})[Ir(TeCl_4)(TeCl_3)]_2$ clusters (Figure 2 and Supporting Information Figure S1). The central Te_{10} molecule coordinates two Ir^{III} cations, each of which also binds to two terminal chlorido tellurate(II) ligands.

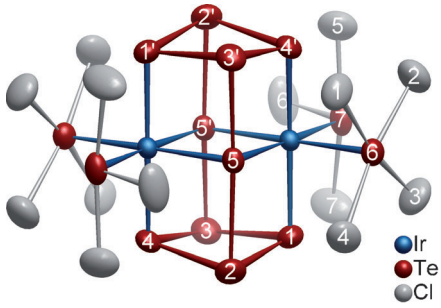

Figure 2. The X-ray structure of the $(Te_{10})[Ir(TeCl_4)(TeCl_3)]_2$ complex (thermal ellipsoids set at 90%) probability.

The biconvex tricyclo[5.1.1.1^{3,5}] unit consists of two Te_4 rings (Te1 to Te4), which are linked through two linear Te bridges (Te5). The Te–Te distances within the folded Te_4 rings (277.88(6)–281.92(6) pm) are slightly longer than the corresponding bonds in the biconcave polycation Te_8^{4+}, tricyclo[3.1.1.1^{3,4}]octatellurium(4+), which does not have the bridging atoms between the rings (Te–Te average 277.4 pm).[10]

In the asymmetric virtually linear fragment Te2-Te5-Te3′ the distances are much longer [Te2–Te5 293.73(5), Te5–Te3′ 307.17(5) pm; bond angle 172.78(1)°]. This roughly corresponds to a 3c–4e bonding as discussed for I_3^-.[13] A simple bond-length bond-strength consideration for the linear Te_3 fragment results in bond valences of 0.62 and 0.43.[14] This type of bonding is described qualitatively by a molecular orbital (MO) model, which results in half a bond between each terminal and the central atom and attributes the negative charge to the terminal atoms,[15] or alternatively by the superposition of basically two asymmetrical mesomeric forms (Figure 3, top).

Taking the 3c–4e bonds into account (Figure 3, bottom), the formal charge assignment according to the 8−*N* rule yields that the linearly two-coordinated Te5 are $(2\times{}^1/_2)$-bonded Te^-, the three-coordinate Te2 and Te3 are $(2+{}^1/_2)$-bonded $Te^{0.5+}$, while the two-coordinate Te1 and Te4 are 2-bonded Te^0. In sum, $(Te^{0.5+})_4(Te^0)_4(Te^-)_2$ represents the formally uncharged molecule Te_{10}. An uncharged Te_{10} mol-

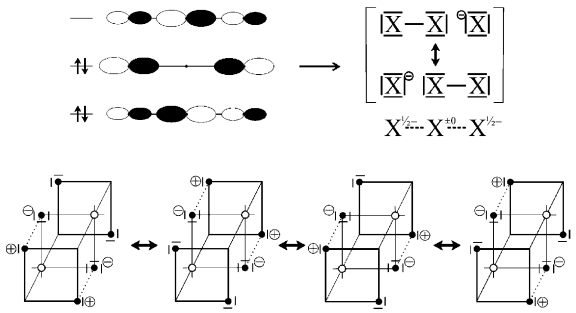

Figure 3. 3c–4e bonds: top: MO scheme and valence bond representation, charges for trihalogenide X_3^- anions, the corresponding tritelluride is Te_3^{4-} with $X = Te^-$; bottom: two resonating 3c–4e bonds in **1**; black spheres: Te of Te_3 units, white spheres: Ir.

ecule is also obtained by applying an alternative way of formal electron counting,[10] in which the linearly coordinated Te5 atoms would have been identified as 2-bonded Te^{2-} atoms and the Te2 and Te3 atoms as 3-bonded Te^+, giving $(Te^+)_4(Te^0)_4(Te^{2-})_2$. This implies a Te^{2-} atom, isoelectronic with Xe, forming two bonds, that is, corresponding to a formal I^- species for the middle atom in I_3^-, not a realistic description.[16] Note, as an effect of the additional homoatomic bonding of the "terminal" Te atoms they become less charged than the middle one, which means a reversal with respect to I_3^- or Te_3^{4-}.[17]

3c–4e bonds are also present in the square-planar $[Te^{+II}Cl_4]^{2-}$ and the T-shaped $[Te^{+II}Cl_3]^-$ groups (Te-Cl 233.8(2)–275.9(2) pm). The Cl atoms that are involved in the longer Te^{II}–Cl bonds interact also with atoms of the Te_{10} molecule ($TeCl_3\cdots$Te: 292.4(1)–332.0(2) pm). Such chlorido tellurate(II) ligands are established parts of rhenium clusters, for example, $[(Re_6Te_8)(Te_6)(TeCl_3)_2]$.[18]

In **1**, each Ir atom is coordinated by four Te atoms of the Te_{10} unit and two of the chlorido tellurate groups; the slightly distorted coordination octahedra are edge-sharing. The Ir–Te distances (263.6(8)–269.1(8) pm) are similar to those in $Ir^{III}Te_2$ (coordination number (c.n.) = 6; 265 pm).[19] Since all coordinating Te atoms act as electron-pair donors, the 18-electron-rule for Ir^{III} is fulfilled and **1** may be formulated as $(Te_{10})^{\pm0}[Ir^{+III}(Te^{+II}Cl_4)(Te^{+II}Cl_3)]_2$.

In line with these considerations, **1** is a diamagnetic semiconductor with a very small band gap of about 0.1 eV (Supporting Information, Figure S3). The magnetic susceptibility shows almost no dependence on the field strength ($0.1\ T \le \mu_0 H \le 7\ T$) in the range from 50 to 400 K (Supporting Information, Figure S4).

Upon heating in an argon stream, **1** decomposes at about 540 K (Supporting Information, Figure S5) according to Equation (1).

$$Ir_2Te_{14}Cl_{14(s)} \rightarrow IrTe_6Cl_{3(s)} + IrCl_{3(s)} + 4\,TeCl_{2(g)} + 2\,Te_{2(s,g)} \quad (1)$$

$[Ir(Te_6)]Cl_3$ is a one-dimensional coordination polymer isostructural to $[Rh(Te_6)]Cl_3$.[6] At higher temperature two further decomposition steps follow that finally yield $IrTe_2$ [Eq. (2) and Supporting Information, Figure S6].

$$IrTe_6Cl_{3(s)} + IrCl_{3(s)} \rightarrow 2\,IrTe_{2(s)} + TeCl_{2(g)} + TeCl_{4(g)} \quad (2)$$

Quantum chemical DFT/B3PW91[20] calculations on an isolated molecule of **1** (experimental structure) have been carried out to investigate the chemical bonding. The bonding analysis was performed in position space applying the topological analysis of the electron density, which yields the QTAIM (Quantum Theory of Atoms in Molecules[21]) atomic basins, as well as of the electron localizability indicator (ELI-D),[22] which yields bond and lone-pair basins. For the present case of a monodeterminantal non-spin-polarized wavefunction ELI-D displays identical locations and types of critical points (e.g. local maxima)[22c] as the well known electron localization function ELF.[23] For the analysis of homoatomic Te bonding the delocalization index between the QTAIM atoms has been employed.[24] It represents the position space analogue to the bond order definition of the Wiberg and the Mayer bond index.[25]

Six local ELI-D maxima (attractors) in the valence region between the Ir and its six coordinating Te atoms confirm covalent Ir–Te bonds (Figure 4). The location of the ELI-D attractors inside the QTAIM Te atoms indicate that the bond is of the polar dative type Te→Ir. For the QTAIM-guided ELI based oxidation number (ELIBON)[26] of Ir only the electronic population of the inner shells are to be counted, while the electronic populations of the donated Te lone pairs are completely assigned to the corresponding Te atom.

With 15.0 electrons found in the fifth atomic shell of Ir, an ELIBON of +2.0 is obtained. Taking into account the ELIBON of +1.6 calculated for $[Ir^{III}Cl_6]^{3-}$ (O_h symmetry, d(Ir–Cl) = 249 pm, low spin, optimized using DFT/B3PW91 and the same basis sets as for the title compound), which clearly indicates a strong tendency of incomplete charge transfer from the penultimate shell region, an ELIBON of 2.0 lies within the range expected for an Ir atom in oxidation state +III.

The fractions of the basin populations of the donated Te lone pairs inside the QTAIM Ir atom (from the ELI-D/QTAIM intersection procedure[27]) are 20 to 23%, which indicates a rather polar bond.[27] The total amount of charge donated from the Te lone pairs to the Ir^{III} cation amounts to 2.4 electrons.

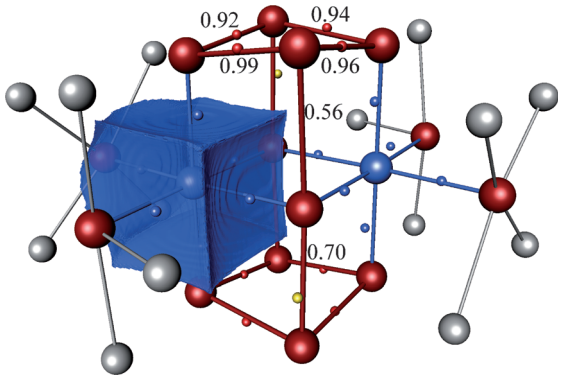

Figure 4. Chemical bonding in **1**. ELI-D attractors for Te–Ir (small blue spheres) and Te–Te bonds (red, yellow). The QTAIM basin of Ir (blue, transparent) does not contain Te–Ir ELI-D attractor. DI values for Te–Te bonds are given for each unique Te–Te bond.

Of the coordinating Te atoms, Te5 is the electron-richest one ($Q_{eff} = +0.37$), closely followed by Te1 and Te4 ($Q_{eff} = +0.44$ and $+0.51$), and finally Te7 and Te6 of the chlorido tellurate groups ($Q_{eff} = +1.10$ and $+1.11$). This sequence is in accord with the above assigned oxidations states. Te2 and Te3, which do not coordinate Ir, are the least-charged Te atoms ($Q_{eff} = +0.10$ and $+0.19$), which is not in contradiction to the (8-*N*)-type counting, since that method neglects coordinative E→M bonding.

The 2c–2e bonds within the Te_4 ring are clearly indicated by ELI-D attractors, while the potential 3c–4e bonding in the linear Te_3 fragment represents difficult terrain for the pure ELI-D bonding analysis at the applied DFT level due to the fractional bond order and substantial electrostatic contributions.[16] For the prototypical 3c–4e bond in the symmetric I_3^- ion only a shallow ELI-D attractor (with very small negative curvatures in transverse directions) close to the terminal atom is found. Upon slight asymmetric distortions these attractors may easily vanish, also depending on the DFT functional used (see the Supporting Information). The functional B3PW91 selected for the present investigation displays an ELI-D attractor only for the shorter Te2–Te5 bond.[28] Full geometry optimization (DFT/BLYP) of molecule **1** results in a structure of D_{2h} symmetry (structure **1′**, Supporting Information, Figure S7) with a 45° rotation of the initial $TeCl_4$ unit around the Ir–Te6 bond axis such that the Cl2 atom becomes symmetrically bridging between Te6 and Te7. This variant may be disfavored in the solid by packing effects. For the present discussion, the most important structural effect is the symmetrization of the 3c–4e bond with d(Te–Te) = 308 pm. Even after relaxation of this structure with the B3PW91 functional (structure **1″**), which shortens the 3c–4e bonds to 299 pm, the ELI-D still does not display the expected local maxima for the 3c–4e bonds. This may be a correlation deficiency at the decisive spatial region, where the ELI-D maximum is expected to occur.

A topological alternative for the definition of an effective covalent bond order is the delocalization index (DI) between the QTAIM atoms.[24] The value of the DI is calculated from integrals over macroscopic spatial regions (the QTAIM atoms) and can be expected to suffer less from local correlation defects. Indeed, it has been successfully applied in a systematic position space study on 3c–4e bonding to the symmetrical Cl_3^- ion at DFT/B3LYP level of theory where a DI of $\delta(Cl_{term}\text{-}Cl_{mid}) = 0.79$ has been obtained.[30] For the Te_3 fragments in **1** slightly smaller values are found with δ(Te2–Te5) = 0.70 and δ(Te5–Te3′) = 0.56 (Figure 4), which resemble the bond valences reported above. For the optimized structure **1″** the symmetrical 3c–4e bonds yield δ(Te2–Te5) = 0.65. The notion of a 3c–4e scenario is additionally corroborated by the comparably high DI δ(Te2-Te3′) = 0.14 (0.15 for **1″**). For the covalent 2c–2e bonds in the Te_4 rings DIs between 0.92 and 0.99 are found in **1** (0.93 in **1″**). Therefore, the Te_{10} molecule can definitely be identified as an entity inside molecule **1**.

Nonetheless, the Ir atoms play the decisive role of stabilizing the Te_{10} unit. An optimization (DFT/B3PW91) of the D_{2h}-symmetric Te_{10} fragment taken from **1′** results in a vibrationally unstable molecule of similar structure with virtually linear 3c–4e bonds and d(Te2–Te5) = 291 pm (Supporting Information, Figure S7). The effective charges are no longer influenced by Ir coordination and follow the conceptual trend given in Figure 3 (bottom), namely Q_{eff} (2.5b)$Te^{0.5+}$ > (2b)Te^0 > (1b)Te^- with values of $+0.09 > -0.05 > -0.08$. The same optimization starting from the experimental structure (C_i symmetry) leads to the disruption of the 3c–4e bonds leaving two identical neutral Te_5 molecules that consist of a Te_4 ring with an exo Te–Te bond (Supporting Information, Figure S7), that is, $(Te^0)_3(Te^+)(Te^-)$. Thus, the Ir atoms specifically enforce the geometry and the electronic structure of the Te_{10} ligand to give the observed 3c–4e bonding.

Experimental Section

The starting materials were handled in an argon filled glove box (M. Braun; $c(O_2) < 1$ ppm, $c(H_2O) < 1$ ppm). Black crystals of **1** were obtained in high yield by for the reaction of a mixture of Ir (99.9%, Chempur), Te (99.999%, Fluka), and $TeCl_4$ (99.9%, Strem, sublimated twice) in the molar ratio 1:5.6:2.6 in a fused evacuated quartz glass ampoule ($l = 120$ mm, $d = 15$ mm). The ampoule was heated to 250 °C within 12 h, left at this temperature for about seven days, and finally cooled to room temperature within 12 h. The excess of $TeCl_4$ was removed by washing with absolute ethanol. The compound is stable in air and inert to water and alcoholic solvents.

The powder diffraction pattern (Supporting Information, Figure S2) was measured using a STOE STADI P powder diffractometer, equipped with a position sensitive detector, and using $Cu_{K\alpha 1}$ radiation ($\lambda = 154.056$ pm). Intensity data were collected with a Bruker AXS Kappa APEX II and $Mo_{K\alpha}$ radiation ($\lambda = 71.073$ pm) at 293(2) K. Numerical absorption corrections[31] based on an optimized crystal description were applied.[32] Structure solution with direct methods[33] was followed by refinements against F_o^2 including anisotropic displacement parameters for all atoms (Supporting Information, Table S1). Structure graphics were generated with Diamond.[34]

1: $[Ir_2(Te_{10})](TeCl_4)_2(TeCl_3)_2$: triclinic, space group $P\bar{1}$ (No. 2), $a = 916.30(7)$, $b = 1002.16(7)$, $c = 1125.92(9)$ pm, $\alpha = 69.34(0)°$, $\beta = 66.94(1)°$, $\gamma = 66.86(1)°$, $V = 850.23(1) \times 10^6$ pm^3; $Z = 1$; $\rho_{calcd} = 5.21$ g cm^{-3}; $\mu(MoK_\alpha) = 20.7$ mm^{-1}; $2\theta_{max} = 71.98°$; 27373 measured, 7954 unique reflections, $R_{int} = 0.066$, $R_\sigma = 0.057$; 137 parameters; extinction parameter $x = 1.5(1) \times 10^{-5}$; $R_1(5864\ F_o > 4\sigma(F_o)) = 0.036$, wR_2(all F_o^2) = 0.054, GooF = 1.15; min./max. residual electron density: $-2.68/2.54$ e × 10^{-6} pm^{-3}.

Further details on the crystal structure investigations may be obtained from the Fachinformationszentrum Karlsruhe, 76344 Eggenstein-Leopoldshafen, Germany (fax: (+49) 7247-808-666; e-mail: crysdata@fiz-karlsruhe.de), on quoting the depository number CSD-422863.

The quantum chemical calculations have been performed on the molecular entity $[Ir_2Te_{14}Cl_{14}]$ which comprises the unit cell and which is not coordinated by atoms from neighboring unit cells. Full structure optimization of the $Ir_2Te_{14}Cl_{14}$ molecule, starting from the experimental structure, was performed with the ADF program[35] at the scalar relativistic ZORA approach[36] employing the DFT/BLYP functional[37] and the all-electron frozen-core (Ir: [Kr]4d^{10}, Te: [Kr], Cl: [Ne]) basis sets of TZ2P quality. The wavefunction for the experimental structure was obtained from a single-point DFT/B3PW91[20] calculation with the Gaussian program[38] employing (quasi)relativistic small-core pseudopotentials and basis sets: Ir ECP-60MWB with (8s7p6d2f)/[6s5p3d2f] basis set,[39] Te ECP-28MDF with VTZ (12s11p9d1f)/[5s4p3d1f] basis set,[40] and Cl ECP-MWB10 and (4s5p)/[2s3p] basis set.[41] DFT/B3PW91 optimizations[38] of a preoptimized (DFT/BLYP, see above) structure of $Ir_2Te_{14}Cl_{14}$ as well as of

the Te_{10} fragment taken from the experimental structure **1** were performed with the same basis sets and pseudopotentials. Exploratory DFT/B3PW1 and BLYP calculations on symmetric I_3^- (structure optimization and single-point calculations of linear-distorted variants with subsequent QTAIM, ELI-D and DI analysis, see Supporting Information) were performed using the I ECP-28MDF with VTZ (15s13p11d1f)/[5s4p3d1f] basis set.[42] In a comparative study, the selected functional B3PW91 has proven to be the most suitable for the calculation of geometry and spectroscopic constants of I_2 and I_3^-.[43] ELI-D and electron density were calculated on an equidistant grid with a mesh size of 0.05 Bohr using DGrid.[44] The topological analysis of both scalar fields, the integration of the electron density in the basins, the ELI-D/QTAIM basin intersection, and the calculation of the DI have been performed with DGrid as well.

Received: April 4, 2011
Revised: May 27, 2011

Keywords: cluster compounds · iridium · multi-center bonding · quantum-chemical calculations · tellurium

[1] W. S. Sheldrick, M. Wachhold, *Angew. Chem.* **1995**, *107*, 490 – 492; *Angew. Chem. Int. Ed. Engl.* **1995**, *34*, 450 – 451.
[2] W. S. Sheldrick, M. Wachhold, *Chem. Commun.* **1996**, 607 – 608.
[3] O. Blacque, H. Brunner, M. M. Kubicki, B. Nuber, B. Stubenhofer, J. Wachter, B. Wrackmeyer, *Angew. Chem.* **1997**, *109*, 361 – 363; *Angew. Chem. Int. Ed. Engl.* **1997**, *36*, 352 – 353.
[4] Yu. Mironov, M. A. Pell, J. A. Ibers, *Angew. Chem.* **1996**, *108*, 2999 – 3001; *Angew. Chem. Int. Ed. Engl.* **1996**, *35*, 2854 – 2856.
[5] H. J. Deiseroth, M. Wagener, E. Neumann, *Eur. J. Inorg. Chem.* **2004**, 4755 – 4758.
[6] A. Günther, A. Isaeva, A. I. Baranov, M. Ruck, *Chem. Eur. J.* **2011**, *17*, 6382 – 6388.
[7] a) C. Graf, A. Assoud, O. Mayasree, H. Kleinke, *Molecules* **2009**, *14*, 3115 – 3131; b) D. M. Smith, J. A. Ibers, *Coord. Chem. Rev.* **2000**, *200 – 202*, 187 – 205.
[8] a) B. Eisenmann, H. Schwerer, H. Schäfer, *Mater. Res. Bull.* **1983**, *18*, 383 – 387.
[9] A. C. Hillier, S. Liu, A. Sella, M. R. J. Elsegood, *Angew. Chem.* **1999**, *111*, 2918 – 2920; *Angew. Chem. Int. Ed.* **1999**, *38*, 2745 – 2747.
[10] a) J. Beck, *Coord. Chem. Rev.* **1997**, *163*, 55 – 70; b) S. Brownridge, I. Krossing, J. Passmore, H. D. B. Jenkins, H. K. Roobottom, *Coord. Chem. Rev.* **2000**, *197*, 397 – 481.
[11] R. Kniep, D. Mootz, A. Rabenau, *Z. Anorg. Allg. Chem.* **1976**, *422*, 17.
[12] R. Kniep, H. Beister, *Angew. Chem.* **1985**, *97*, 399 – 400; *Angew. Chem. Int. Ed. Engl.* **1985**, *24*, 393 – 394.
[13] P. H. Svensson, L. Kloo, *Chem. Rev.* **2003**, *103*, 1649 – 1684.
[14] N. E. Brese, M. O'Keeffe, *Acta Crystallogr. Sect. B* **1991**, *47*, 192 – 197.
[15] a) G. C. Pimentel, *J. Chem. Phys.* **1951**, *19*, 446 – 448; b) R. J. Hach, R. E. Rundle, *J. Am. Chem. Soc.* **1951**, *73*, 4321 – 4324.
[16] G. A. Landrum, N. Goldberg, R. Hoffmann, *J. Chem. Soc. Dalton Trans.* **1997**, 3605 – 3613.
[17] P. Böttcher, *Angew. Chem.* **1988**, *100*, 781 – 794; *Angew. Chem. Int. Ed. Engl.* **1988**, *27*, 759 – 772.
[18] Y. V. Mironov, V. E. Fedorov, *J. Struct. Chem.* **2000**, *40*, 959 – 974.
[19] E. F. Hockings, J. G. White, *J. Phys. Chem.* **1960**, *64*, 1042 – 1045.
[20] a) A. D. Becke, *J. Chem. Phys.* **1993**, *98*, 5648 – 5652; b) J. P. Perdew, J. A. Chevary, S. H. Vosko, K. A. Jackson, M. R. Pederson, D. J. Singh, C. Fiolhais, *Phys. Rev. B* **1992**, *46*, 6671 – 6687.
[21] R. F. W. Bader, *Atoms in Molecules: A Quantum Theory*, Oxford University Press, Oxford, **1994**.
[22] a) M. Kohout, *Int. J. Quantum Chem.* **2004**, *97*, 651 – 658; b) M. Kohout, *Faraday Discuss.* **2007**, *135*, 43 – 54; c) F. R. Wagner, V. Bezugly, M. Kohout, Yu. Grin, *Chem. Eur. J.* **2007**, *13*, 5724 – 5741; d) F. R. Wagner, M. Kohout, Yu. Grin, *J. Phys. Chem. A* **2008**, *112*, 9814 – 9828.
[23] A. D. Becke, K. D. Edgcombe, *J. Chem. Phys.* **1990**, *92*, 5397 – 5403.
[24] a) J. G. Angyan, M. Loos, I. Mayer, *J. Phys. Chem.* **1994**, *98*, 5244 – 5248; b) R. F. W. Bader, A. Streitwieser, A. Neuhaus, K. E. Laidig, P. Speers, *J. Am. Chem. Soc.* **1996**, *118*, 4959 – 4965; c) X. Fradera, M. A. Austen, R. F. W. Bader, *J. Phys. Chem. A* **1999**, *103*, 304 – 314.
[25] a) K. Wiberg, *Tetrahedron* **1968**, *24*, 1083 – 1096; b) I. Mayer, *Chem. Phys. Lett.* **1983**, *97*, 270 – 274.
[26] a) I. Veremchuk, T. Mori, Yu. Prots, W. Schnelle, A. Leithe-Jasper, M. Kohout, Yu. Grin, *J. Solid State Chem.* **2008**, *181*, 1983 – 1991; b) P. Höhn, S. Agrestini, A. Baranov, S. Hoffmann, M. Kohout, F. Nitsche, F. R. Wagner, R. Kniep, *Chem. Eur. J.* **2011**, *17*, 3347 – 3351.
[27] a) G. Jansen, M. Schubart, B. Findeis, L. Gade, I. J. Scowen, M. McPartlin, *J. Am. Chem. Soc.* **1998**, *120*, 7239 – 7251; b) S. Raub, G. Jansen, *Theor. Chem. Acc.* **2001**, *106*, 223 – 232.
[28] The appropriate solution for such correlation problems would be the use of multiconfigurational MCSCF or CAS methods. The combination of these wavefunction-based methods with position-space bonding indicators like ELI-D has recently been demonstrated for the eight dimers Li_2 to Ne_2.[29]
[29] a) V. Bezugly, M. Kohout, F. R. Wagner, *J. Comput. Chem.* **2010**, *31*, 1504 – 1519; b) V. Bezugly, M. Kohout, F. R. Wagner, *J. Comput. Chem.* **2010**, *31*, 2273 – 2285.
[30] J. Molina Molina, J. A. Dobado, *Theor. Chem. Acc.* **2001**, *105*, 328 – 337.
[31] Stoe & Cie GmbH, *X-RED 32 1.01*, *Data Reduction Program*, Darmstadt, Germany, **2001**.
[32] Stoe & Cie GmbH, X-SHAPE 1.06, Crystal Optimisation for Numerical Absorption Correction Program, Darmstadt, Germany, **1999**.
[33] G. M. Sheldrick, *Acta Crystallogr. Sect. A* **2008**, *64*, 112 – 122.
[34] K. Brandenburg, *Diamond 3.2g*, *Crystal and Molecular Structure Visualization*, Crystal Impact GbR, Bonn, Germany, **2011**.
[35] ADF2009.01, SCM, Theoretical Chemistry, Vrije Universiteit, Amsterdam, The Netherlands, http://www.scm.com.
[36] a) E. van Lenthe, E. J. Baerends, J. G. Snijders, *J. Chem. Phys.* **1993**, *99*, 4597 – 4610; b) E. van Lenthe, E. J. Baerends, J. G. Snijders, *J. Chem. Phys.* **1994**, *101*, 9783 – 9792; c) E. van Lenthe, A. E. Ehlers, E. J. Baerends, *J. Chem. Phys.* **1999**, *110*, 8943 – 8953.
[37] a) A. D. Becke, *Phys. Rev. A* **1988**, *38*, 3098 – 3100; b) C. Lee, W. Yang, R. G. Parr, *Phys. Rev. B* **1988**, *37*, 785 – 789.
[38] M. J. Frisch et al., Gaussian 09, Revision A.02, Gaussian, Inc., Wallingford, CT, **2009** (full citation: see Supporting Information,).
[39] a) D. Andrae, U. Häussermann, M. Dolg, H. Stoll, H. Preuss, *Theor. Chim. Acta* **1990**, *77*, 123 – 141; b) J. M. L. Martin, A. Sundermann, *J. Chem. Phys.* **2001**, *114*, 3408 – 3420.
[40] K. A. Peterson, D. Figgen, E. Goll, H. Stoll, M. Dolg, *J. Chem. Phys.* **2003**, *119*, 11113 – 111123.
[41] A. Bergner, M. Dolg, W. Küchle, H. Stoll, H. Preuss, *Mol. Phys.* **1993**, *80*, 1431 – 1441.
[42] K. A. Peterson, B. C. Shepler, D. Figgen, H. Stoll, *J. Phys. Chem. A* **2006**, *110*, 13877 – 13883.
[43] S. B. Sharp, G. I. Gellene, *J. Phys. Chem. A* **1997**, *101*, 2192 – 2197.
[44] M. Kohout, *DGrid 4.6*, Radebeul (Germany), **2011**.

